Journal of Magnetic Resonance 202 (2010) 234–238

Contents lists available at ScienceDirect

Journal of Magnetic Resonance

journal homepage: www.elsevier.com/locate/jmr

Variable bandwidth filtering for magnetic resonance imaging with pure phase encoding

Juan C. García-Naranjo [a,b,c], Paul M. Glover [d], Florin Marica [a], Bruce J. Balcom [a,*]

[a] MRI Centre, Department of Physics, P.O. Box 4400, University of New Brunswick, Fredericton, NB, Canada E3B 5A3
[b] Department of Electrical and Computer Engineering, P.O. Box 4400, University of New Brunswick, Fredericton, NB, Canada E3B 5A3
[c] Centre of Medical Biophysics, Universidad de Oriente, Patricio Lumumba S/N, Santiago de Cuba 90500, Cuba
[d] The Sir Peter Mansfield Magnetic Resonance Centre, School of Physics and Astronomy, University of Nottingham, Nottingham NG7 2RD, UK

ARTICLE INFO

Article history:
Received 5 December 2008
Revised 23 October 2009
Available online 18 November 2009

Keywords:
MRI
SPRITE
Pure phase encoding
Filtering
Variable bandwidth filter
SNR

ABSTRACT

Magnetic resonance imaging with pure phase encoding (sometimes known as single point or constant time imaging) has many desirable advantages, but is usually time consuming in comparison to frequency encoding methods. In single point imaging the maximum signal bandwidth is proportional to both the phase-encoding gradient amplitude and the object size. It is usual practice to set the acquisition filter bandwidth to the maximum value expected during a measurement. Hence the filtering employed in this kind of measurement is not optimal for the low frequency *k*-space points. An optimal way to set the filter bandwidth is presented in this study. By reducing the filter bandwidth to match the point sampled in *k*-space, the inherent SNR is improved and this, in turn, may be used to reduce the number of signal averages required for acceptable SNR. The variable bandwidth filter offers a theoretical SNR increase of 41%. This paper shows the results of its application and comparison with fixed low-pass filtering. Practical measurements show a gain of 20% in SNR, which would translate into a 31% reduction in averaging time required for a single image without any detrimental effects on the image quality.

1. Introduction

Magnetic resonance with pure phase encoding has been employed for approximately twenty years in different applications, mainly related to the study of solid-like samples and porous media [1–7]. Because of the fixed encoding time t_p, the magnetization time evolution is not measured. Instead spatial information is encoded by changing the amplitude of the applied gradient and a different *k*-space point is sampled for each RF pulse. Single point methods are largely immune to artifacts caused by magnetic field inhomogeneities, chemical shift, and dipolar and quadrupolar distortions [2].

Nevertheless, pure phase encode measurements are inherently less sensitive than frequency encoding due to the fact each excitation results in acquisition of only a single *k*-space point. Balcom et al. introduced the SPRITE measurement which demonstrated a dramatic reduction in the time of experiment [3]. However, SPRITE is still inefficient compared to frequency encoding and additional strategies to improve the inherent SNR are desirable. Eliminating or reducing the necessity of signal averaging is critical to speeding up the technique.

Romanenko et al. [4] have introduced a variable flip angle excitation scheme for increased sensitivity in SPRITE MRI with very good results. A second complementary approach is presented in this paper, focused on the filtering process in the SPRITE measurements.

Conventional filtering, employed in pure phase MRI experiments, is inefficient. The central *k*-space points, with narrow signal bandwidth, are filtered using a fixed low-pass filter set according to the bandwidth of peripheral *k*-space points. This study introduces a new way of filtering for pure phase encoding sequences using a variable bandwidth filter (VBF). Practical measurements show a gain of 20% in SNR in comparison with conventional fixed low-pass filtering, which would translate into a 31% reduction in the duration of the experiment (if limited by SNR), without other effects on the original image.

2. Theory

2.1. Pure phase encoding experiment

In pure phase encoding measurements, as in SPRITE (see Fig. 1), magnetization evolution for a fixed time with different gradient strengths is employed to acquire data points in *k*-space. The *n*th sampled *k*-space point (commencing at the origin) is given by,

* Corresponding author. Fax: +1 506 453 4581.
E-mail address: bjb@unb.ca (B.J. Balcom).

1090-7807/$ - see front matter © 2009 Elsevier Inc. All rights reserved.
doi:10.1016/j.jmr.2009.11.006

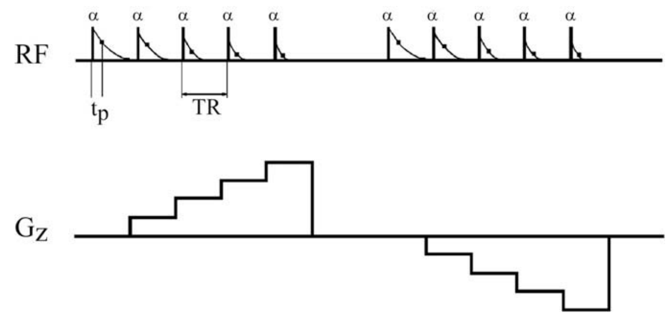

Fig. 1. SPRITE pulse sequence. A one dimensional phase-encoding gradient (G_z) is employed to obtain a sample profile. A single FID point is sampled at a time t_p after each RF pulse (α).

$$k_n = \frac{\gamma n \Delta G t_p}{2\pi}, \tag{1}$$

where ΔG is the fixed gradient increment between RF pulses. For each k-space point a new gradient value and RF excitation pulse is applied and, after a fixed encoding time t_p, a single data point is acquired. In the proposed scheme the signal bandwidth will increase proportional to k_n in progressing from the centre to the extreme of k-space. The low-pass filter width *FW* should normally be set according to the maximum applied gradient amplitude,

$$FW \geqslant \frac{|G_{\max}|}{2 t_p \Delta G}, \tag{2}$$

as given by Gravina and Cory [2]. The signal from the central points of k-space, which have narrow bandwidth *BW* given by,

$$BW = \frac{n}{2 t_p}, \tag{3}$$

will incorporate noise and be filtered inefficiently. An optimal solution will involve the use of a filter with variable bandwidth linked to the k-space sample index. This means that for each gradient step a new filter width should be applied.

2.1. Variable bandwidth filter

The simplest way to examine the VBF is to consider noise in the signal as white noise (as is the case for thermal sources), with an ideal transfer function of the low-pass filter having $|H(f)| = 1$ in the pass-band, $|H(f)| = 0$ in the stop-band [8,9]. In this case, because the noise power spectral density is constant over the whole bandwidth, the reduction in noise power will be directly related to the selected bandwidth. Therefore, changing the filter width according to the signal bandwidth will result in a decrease in the noise power from the extremities of k-space, where the bandwidth is wide, to the centre where it is very narrow. This means that in the filtered k-space the ideal power spectral density function (Φ_n) will follow a linear variation, directly proportional to the k-space sample index (Fig. 2). Therefore, it should be possible to remove one half of the noise power in the k-space data, which means an increase of $\sqrt{2}$ in SNR of the profile.

In SPRITE the maximum encoding bandwidth increases with each added dimension because of the linear superposition of the gradients. For 2D the required filter width *FW* is,

$$FW = \frac{\gamma}{2}\left(FOV_x|G_{x\max}| + FOV_y|G_{y\max}|\right) \tag{4}$$

The filter width for 2D is therefore twice that of 1D for a square *FOV*. Similar analysis can be undertaken for 3D with similar results. The conclusion is always the same, namely that the maximum overall increase in SNR available is $\sqrt{2}$.

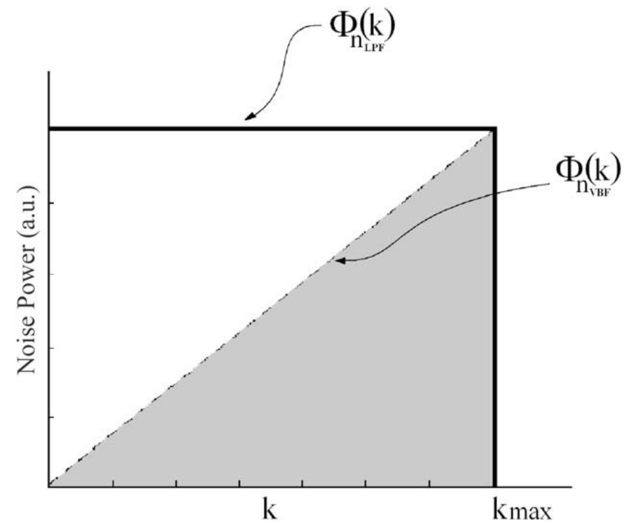

Fig. 2. Power spectral density of ideal white noise $\Phi_n(k)$ resulting from the filtering process using an ideal low-pass filter. The shaded area represents the power spectral density when the VBF is applied. Ideally one half of the noise power from the k-space data should be removed, which means an increase of $\sqrt{2}$ in SNR for the profile.

One usually assumes that the SNR in an acquisition will be directly proportional to the square root of the number of averages [10]. Therefore, the gain in SNR using VBF is the same as two signal averages using classical low-pass filtering. In other words, VBF offers a potential reduction of 50% in time for a SPRITE experiment with fixed SNR.

In the practical implementation of VBF, a zero-phase filter (zero delay) [8,9] is required in order to avoid problems with phase modulation of k-space. This type of (non-causal) filtering is physically unrealizable [8] and is only possible with offline processing [11]. Even when this phase modulation can be corrected, because the parameters of the VBF are known, this would introduce an additional and unnecessary complexity to the filtering algorithms. Therefore, for real time applications it is very important to maintain the same delay for all frequency components. This means that all the filters must have the same order and the sampling frequency must be constant and independent of the bandwidth [8,9]. Hence, even for VBF, the data must be acquired with a significantly higher bandwidth than would usually be the case.

We anticipate very efficient filtering at the k-space origin, which should improve SNR. In reality the filter cannot be set to zero and is subject to a minimum constraint dependent on t_p and system dead-time. In addition the VBF will be less efficient at the k-space periphery, which controls fine details in the image.

Ideal behavior is of course not always observed for real electronic systems [12]. Hence, it is not possible to evaluate the true VBF performance in advance. Therefore, this study presents the result of applying 28 VBF filter widths in a 64 point centre-out double half k-space acquisition. This result is compared with a classical fixed low-pass filtered image. Each filter width was applied in both half k-spaces, resulting in 56 VBF filtered k-space points during the whole acquisition process to obtain the filtered profile.

3. Results and discussion

Fig. 3 shows four filter widths of the VBF obtained with the parameters and proposed algorithm; the pass-band attenuation is 0 dB and, more than 60 dB in the stop-band. For the central k-space point, where no gradient is applied, a very narrow filter could be employed making very efficient the VBF in this area.

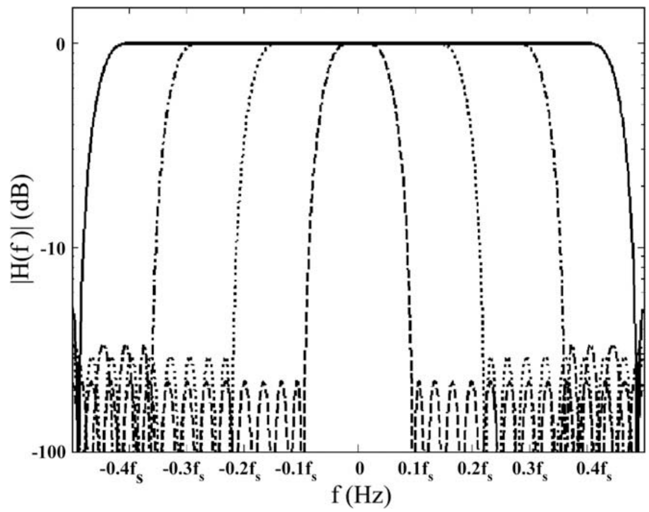

Fig. 3. Transfer function *H(f)* of four VBF filter widths. The filter width is very narrow in the centre of the *k*-space (- -) and wider in the extremity (–). The sampling frequency (f_s) is 1 MHz and the filter order has been fixed to 30.

The only limitation for the filter width at this point is the signal linewidth which is inversely related to T_2^*. Therefore, the more efficient filter will depend on a sample parameter, making the filter setting sample specific which is not desirable. Instead, the minimum filter width was set according to the first non-zero gradient which is related to the image field of view and is therefore size specific. The VBF was not applied to the *k*-space extremity points where classical low-pass filtering was employed.

In the first experiment, a noise only profile was acquired in the absence of sample. The noise voltage with and without VBF was calculated for 40 profiles to measure the noise reduction in each of them. The mean value reduction in all these measurements was 20% with a standard deviation of 8%. One of the noise profiles with and without VBF is illustrated in Fig. 4.

In a second step, the same measurement was carried out over a homogeneous region of one profile from the experimental sample, obtained with the same acquisition and processing parameters of our previous experiment. Fig. 5 shows a comparison between the filtered profile using classical low-pass filtering and VBF. Because of the shape of our sample, the ideal profile should be a boxcar function and any uncertainty will be considered noise. In this case, the gain in SNR is 24% in the homogeneous region (top centre) of the profile, which agrees with the previous result and means a

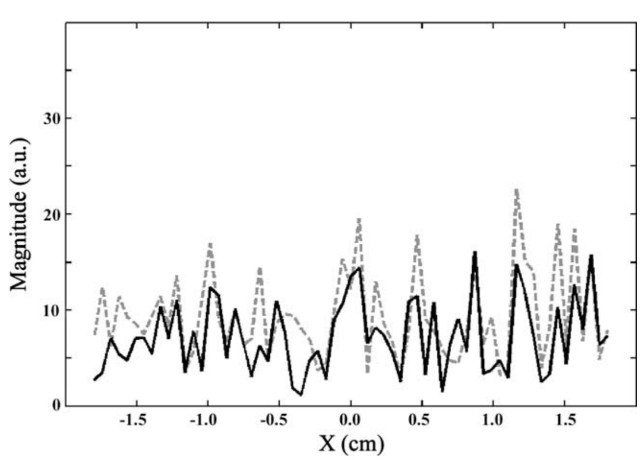

Fig. 4. Image acquisition in the absence of sample using a classical low-pass filter (- -) and VBF (–).

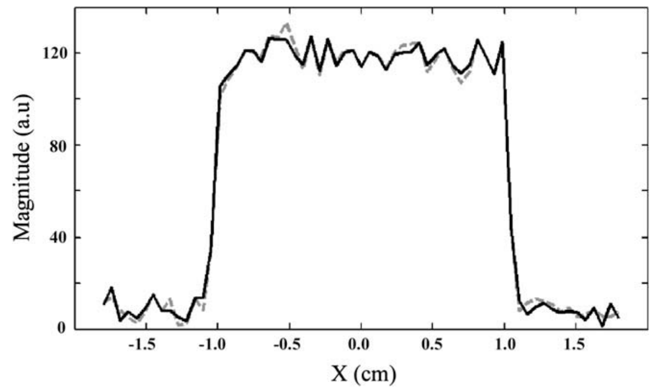

Fig. 5. 1D image obtained with classical low-pass filter (- -) and VBF (–). In this case, the gain in signal to noise was 24%, which means a reduction of 35% in the time of experiment. VBF does not affect the sharp edges in the profile.

reduction of 35% in the time of experiment. As can be observed, the VBF has no deleterious effects on the profile shape.

The filter width of the classical low-pass filter was set for 500 kHz, which is wider than the optimal value (81.6 kHz), to be able to acquire 128 points for post processing. The filter widths of the VBF have been designed according to the bandwidth of the classical low-pass filter and the number of gradient steps. Wider low-pass filter will imply wider VBF filter widths. Therefore, the noise reduction, as a relative measurement, will be independent of the bandwidth.

The observed difference between the ideal SNR gain (40%) and the experimental realization (20%) can be explained from a critical analysis of the experiment assumptions.

In the ideal case, zero filter width in the *k*-space origin was assumed. Nevertheless, in practical implementations of VBF the minimum filter width was set according to the lowest gradient value different from zero, which is wider than the signal linewidth. This reduces the filtering effectiveness in the centre of the *k*-space, shifting up the ideal noise distribution (Fig. 6), but makes the VBF independent of the sample.

In general, the white noise condition is not achieved because of the combination of different noise sources in electronic devices,

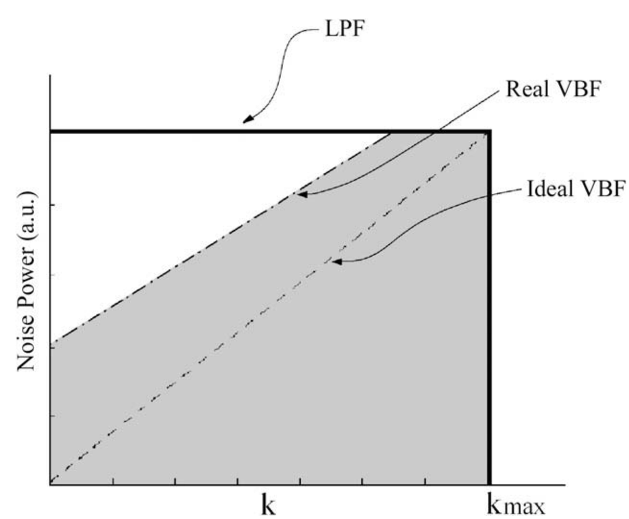

Fig. 6. Descriptive representation of the influence of real factors on the ideal VBF performance of Fig. 2. Wider filter width in the centre of *k*-space and noise in electronic systems (non-ideal) shift up the ideal line in the centre of *k*-space. Unfiltered *k*-space extremity points shift it left. The non-ideal transition band of the VBF filter widths contribute to both effects.

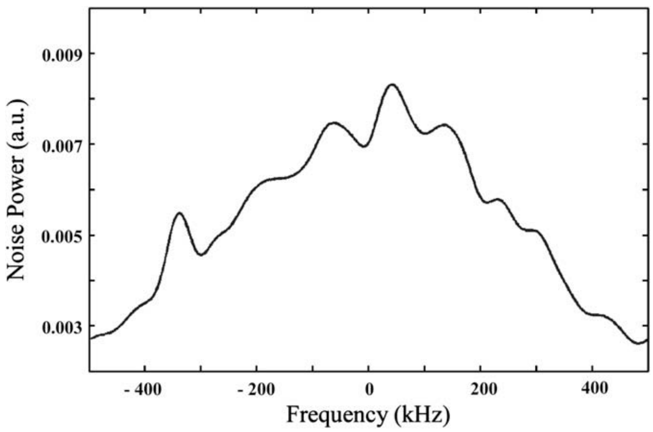

Fig. 7. Noise power spectral density in the receiver channel of MARAN-DRX console. Higher energy concentration in the lower frequencies reduces the effectiveness of the VBF.

most of them in the low frequency band [10,12]. The combination of all these sources will increase the noise energy in the low frequency band and therefore increase the noise in the centre of *k*-space (Fig. 6). The power spectral density of the noise in the receiver system (Fig. 7) obtained from 40 noise acquisitions employing Welch averaging modified periodograms [8] shows this behavior.

In addition, in real cases it is not possible to employ a VBF for the extremity points of *k*-space because the bandwidth is close to the sampling frequency and undesirable aliasing could take place because of the transition band in the non-ideal filter transfer function [9]. This reduces the number of VBF filter widths applied from 32, which is the number of points of one half of the *k*-space, to 28. In these extremity points conventional low-pass filtering was employed. The extremity *k*-space data points will contribute to fine profile structure, but will also reduce the SNR gain by shifting left the ideal noise distribution line in the extremity of *k*-space (Fig. 6). Furthermore, the filter transition band will also increase the noise contribution in comparison to the ideal case (Fig. 6). This characteristic could be improved by increasing the filter order but it will also increase the filter dead-time, which is not desirable for samples with fast T_2^* decay.

Fig. 8 shows the actual *k*-space power spectral density measured using classical low-pass filter and VBF. Similar behavior to the model in Fig. 6 can be observed. Measurements of the area

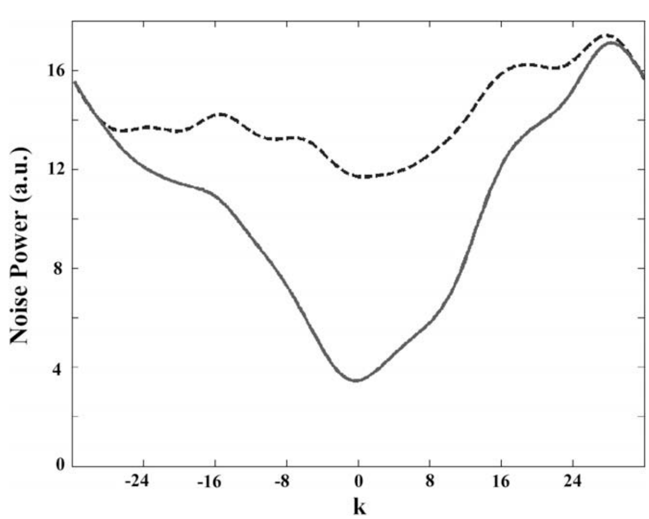

Fig. 8. Bilateral *k*-space power spectral density measured using classical low-pass filter (- -) and VBF (–). The area under the curve is 18% less for VBF.

under both curves show a reduction of 18% for VBF, which agrees with the reported gain in SNR.

The previous analysis can be applied also for 2D or 3D imaging. In SPRITE the maximum encoding bandwidth required increases with each added dimension. Therefore, each dimension will contribute noise that can be removed with VBF, hence the gain in SNR should be equivalent to the 1D experiment for the same field of view in each dimension.

4. Conclusions

A new way to filter pure phase encode MRI data has been presented. By applying a variable bandwidth filter, the SNR for 1D images can be increased by about 20% in comparison to a fixed bandwidth classical low-pass filter. This gain represents a reduction of up to 31% in time of an experiment limited by signal averaging. The persistent sensitivity disadvantage of pure phase encode MRI compared to frequency encode methods means that even a 31% improvement can be significant. Practical measurements also demonstrate conservation of the structural features and resolution in the VBF profile.

5. Experimental

The VBF was applied offline for a 1D MRI image data set. An elastomeric sample of polyvinyl chloride, 2.2 cm in length, 2.2 cm width, with a T_2^* of 380 μs was the test sample during the data acquisition.

The Parks–McClellan algorithm [9] was applied to calculate the VBF coefficients with MATLAB. The filter has order 30 with linear phase response [9]. A sampling frequency of 1 MHz was employed for all the VBF filter widths to maintain the same delay (15 μs) for all *k*-space points. The maximum absolute amplitude error [9] in the band-pass was 0.002 and 0.1 in the stop-band.

MRI data acquisition was performed on a MARAN-DRX 7 T MRI system (Oxford Instruments, UK) operating at a proton frequency of 299.65 MHz, with a 160 mm horizontal bore actively screened magnet. Magnetic field gradients of up to 40 G/cm were provided by a self-shielded gradient set SGRAD 156/100/S (Magnex Scientific, UK). A 6.2 cm diameter home built birdcage RF resonator was used for both radiofrequency transmission and reception. The RF pulse had a duration of 6.2 μs, corresponding to a flip angle of 10°. The 1000 W NMR plus RF power amplifier was provided by Communication Power (Brentwood, NY).

For comparison with VBF the MARAN-DRX console Ultrashape classical low-pass filter was employed. This digital filter has order 13 and a filter width of 500 kHz. Because the VBF has been applied offline, multiple points must be stored. Such data storage is clearly inefficient and ultimately undesirable.

The sample profile was obtained using the SPRITE sequence reproduced in Fig. 1 with an encoding time of 196 μs, a maximum gradient value of 11.6 G/cm and 64 *k*-space points. In each FID, 128 points with a dwell time of 1 μs were collected for post processing. To obtain the filtered profile, 28 VBF filter widths were applied on each half of *k*-space, resulting in 56 VBF filtered points over the whole *k*-space.

Acknowledgments

J.C.G. thanks the Canadian International Development Agency (CIDA) for supporting part of this work. P.M.G. wishes to acknowledge EPSRC of UK for support. BJB thanks NSERC of Canada and the Canada Chairs program for a chair in MRI of materials. The UNB MRI centre is supported by an NSERC Major Resources Support grant.

References

[1] S. Emid, J.H.N. Creyghton, High resolution NMR imaging in solids, Physica 128B (1985) 81–83.

[2] S. Gravina, D.G. Cory, Sensitivity and resolution of constant-time imaging, J. Magn. Reson. B 104 (1994) 53–61.

[3] B.J. Balcom, R.P. MacGregor, S.D. Beyea, D.P. Green, R.L. Armstrong, T.W. Bremner, Single-point ramped imaging with T_1 enhancement (SPRITE), J. Magn. Reson. A 123 (1996) 131–134.

[4] K.V. Romanenko, P.F. de J. Cano-Barrita, Bruce J. Balcom, ^{35}Cl profiling using centric scan SPRITE with variable flip angle excitation, J. Magn. Reson. 198 (2009) 24–30.

[5] B.J. Balcom, J.C. Barrita, C. Choi, S.D. Beyea, D.J. Goodyear, T.W. Bremner, Single-point magnetic resonance imaging (MRI) of cement based materials, Mater. Struct. 36 (2003) 166–182.

[6] L. Li, F. Marica, Q. Chen, B. MacMillan, B.J. Balcom, Quantitative discrimination of water and hydrocarbons in porous media by magnetization prepared centric-scan SPRITE, J. Magn. Reson. 186 (2007) 282–292.

[7] H. Hickey, B. MacMillan, B. Newling, M. Ramesh, P.V. Eijck, B.J. Balcom, Magnetic resonance relaxation measurements to determine oil and water content in fried foods, Food Res. Int. 39 (2006) 612–618.

[8] J.G. Proakis, D.G. Manolakis, Digital Signal Processing, Prentice Hall, New Jersey, 2007. pp. 655–659.

[9] A.V. Oppenheim, R.W. Schafer, Discrete-Time Signal Processing, Prentice Hall, New Jersey, 1989. pp. 476–478.

[10] R.R. Ernst, Sensitivity enhancement in magnetic resonance. I. Analysis of the method of time averaging, Rev. Sci. Instr. 36 (1965) 1689–1695.

[11] F. Gustafsson, Determining the initial states in forward–backward filtering, IEEE Trans. Signal Process. 44 (1996) 988–992.

[12] H.W. Ott, Noise Reduction Techniques in Electronic Systems, John Wiley & Sons, USA, 1988. pp. 228–243.